Vision Research 48 (2008) 1545–1553

Contents lists available at ScienceDirect

Vision Research

journal homepage: www.elsevier.com/locate/visres

The organization of spatial frequency maps measured by cortical flavoprotein autofluorescence

Atul K. Mallik [a], T. Robert Husson [b], Jing X. Zhang [c], Ari Rosenberg [b], Naoum P. Issa [d,*]

[a] Committee on Neurobiology, University of Chicago, USA
[b] Committee on Computational Neuroscience, University of Chicago, USA
[c] Department of Biomedical Engineering, Illinois Institute of Technology, USA
[d] Department of Neurobiology, University of Chicago, 947 E. 58th Street, MC0926, Chicago, IL 60637, USA

ARTICLE INFO

Article history:
Received 14 August 2007
Received in revised form 14 April 2008

Keywords:
Visual cortex
Intrinsic signals
Flavoproteins
Autofluorescence
Cerebral metabolism
Spatial frequency

ABSTRACT

To determine the organization of spatial frequency (SF) preference within cat Area 17, we imaged responses to stimuli with different SFs using optical intrinsic signals (ISI) and flavoprotein autofluorescence (AFI). Previous studies have suggested that neurons cluster based on SF preference, but a recent report argued that SF maps measured with ISI were artifacts of the vascular bed. Because AFI derives from a non-hemodynamic signal, it is less contaminated by vasculature. The two independent imaging methods produced similar SF preference maps in the same animals, suggesting that the patchy organization of SF preference is a genuine feature of Area 17.

1. Introduction

Neurons within primary visual cortex of visual mammals are selective for the spatial frequency (SF) of a stimulus (Campbell, Cooper, & Enroth-Cugell, 1969; Movshon, Thompson, & Tolhurst, 1978; Tolhurst & Thompson, 1982) and neurons with similar SF preference cluster together, as has been shown for other response properties like orientation preference and ocular dominance (Hubel & Wiesel, 1962). Electrophysiological studies have shown that neighboring neurons are more likely than chance to prefer similar SFs (DeAngelis, Ghose, Ohzawa, & Freeman, 1999; Maffei & Fiorentini, 1977; Tolhurst & Thompson, 1982), and on a larger scale, maps of SF preference measured using intrinsic signal imaging (ISI) have suggested that there is an ordered map of SF preference across the surface of cortical Area 17 in the cat (Everson et al., 1998; Hubener, Shoham, Grinvald, & Bonhoeffer, 1997; Issa, Trepel, & Stryker, 2000; Shoham, Hubener, Schulze, Grinvald, & Bonhoeffer, 1997a). However, a recent reanalysis of ISI data has called into question the maps of SF preference, suggesting that these maps represent the vascular structure of visual cortex and not spatial modulation of SF preference (Sirovich & Uglesich, 2004). Based on an additional data set, the authors also suggested that SF preference does not vary in an organized fashion across the tangential extent of Area 17 (Sirovich & Uglesich, 2004).

To determine if SF preference varies systematically across the cortical surface we reinvestigated its organization using flavoprotein autofluorescence imaging (AFI). AFI is a non-hemodynamic measure of cellular metabolism derived from the fluorescence of flavoproteins associated with the electron transport chain in mitochondria (Foster, Galeffi, Gerich, Turner, & Muller, 2006; Reinert, Dunbar, Gao, Chen, & Ebner, 2004; Tohmi, Kitaura, Komagata, Kudoh, & Shibuki, 2006; Turner, Foster, Galeffi, & Somjen, 2007). We have recently shown that AFI produces high-quality images of cortical organization in the cat, with improved spatial and temporal resolution compared to intrinsic signal imaging (Husson, Mallik, Zhang, & Issa, 2007). Because AFI does not rely on blood oxygenation or blood flow changes, it has far fewer vascular artifacts than does ISI (Husson et al., 2007).

AFI maps suggest that SF preference has a clustered organization that varies across the cortical surface of cat Area 17, consistent with previous ISI studies (Everson et al., 1998; Hubener et al., 1997; Issa et al., 2000; Shoham et al., 1997a). Furthermore, the SF preference maps and tuning curves measured by AFI are statistically similar to those produced by ISI in the same animals, suggesting that tangential variation of SF preference is a genuine feature of the organization of primary visual cortex.

2. Materials and methods

All experimental procedures were approved by the University of Chicago Institutional Animal Care and Use Committee. Results from four female cats aged 14 weeks or older are reported. For two of the animals data from different experiments

* Corresponding author. Fax: +1 773 702 3774.
E-mail address: nissa@drugs.bsd.uchicago.edu (N.P. Issa).

0042-6989/$ - see front matter © 2008 Elsevier Ltd. All rights reserved.
doi:10.1016/j.visres.2008.04.014

were reported in (Husson et al., 2007). The surgical procedures are described in detail in Husson et al. (2007), and are briefly summarized here. Cats were anesthetized with thiopental (20–30 mg/kg IV loading dose, 2–10 mg/kg IV, PRN for maintenance). Ophthalmic phenylephrine (10%) and atropine (1%) were instilled in the eyes, and the eyes were focused at 40 cm with contact lenses. Portions of areas 17 and 18 were exposed through a craniotomy and the brain was stabilized with 3% agarose in sterile saline and then covered with a glass coverslip.

2.1. Visual stimuli

Visual stimuli were created using the Psychophysics Toolbox (Brainard, 1997; Pelli, 1997) in MATLAB (The MathWorks, Inc, Natick, MA), and were presented on a 21″ gamma-corrected CRT display (Dell P1230, Round Rock, TX). Data from two of the four animals were collected using an uncorrected monitor, resulting in the inclusion of low amplitude harmonics (a Fourier transform of the stimulus shows a second-harmonic with an amplitude of 12% that of the fundamental's amplitude, and a third harmonic with an amplitude of 4%); results from these two animals are reported separately in supplementary figures. The stimuli were viewed binocularly from 40 cm. To generate SF maps, sine wave gratings were presented at four orientations (0°, 45°, 90°, 135°) and six spatial frequencies (0.1, 0.25, 0.5, 0.75, 1.0, 1.5 c/°) in pseudo-random order. All gratings were presented at 80% contrast, and drifted across the central 60° of visual space at a temporal frequency of 2 c/s. Each stimulus was initially stationary for 6 s, and then drifted for 6 s. Drift direction reversed every 2 s. Each stimulus set included four randomly interleaved mean-luminance gray stimuli; the responses averaged over these four stimuli were used to produce a "blank" response image. Images were collected over the last 5.5 s of each stimulus presentation, and were averaged over 16 or 32 presentations of each stimulus.

2.2. Optical imaging

Images were obtained using a Dalsa 1M30 camera (Dalsa Corp, Waterloo, Ontario, Canada) mounted on a macroscope (Bonhoeffer & Grinvald, 1996) with 50 mm lenses (1.4 f, Nikon, Melville, NY) and controlled by a custom LabVIEW (National Instruments, Austin, TX) interface. The cortex was illuminated with two 12 W light sources (Oriel, Richmond, CA) through fiber optic cables. For ISI, the cortex was illuminated with 610 ± 10 nm light with a matched filter (Newport, Stratford, CT) in front of the CCD camera and images were acquired at 30 frames per second, temporally averaged over four images, and spatially binned after acquisition (2 × 2 bins). For AFI, fluorescence was excited with 420–490 nm light and the emitted light was long-pass filtered above 515 nm (Chroma, Rockingham, VT). Images were acquired at 5–10 fps with no temporal or software binning, but with 2 × 2 on-chip spatial binning.

2.3. Image analysis

AFI and ISI images were analyzed using custom software in the IDL environment (ITT Visual Information Solutions, Boulder, CO). To produce single-condition images, we first normalized the average response for a given condition to the response to a blank screen ("blank normalization"). Both AFI and ISI images were then spatially high-pass filtered by first generating a smoothed image with a moving window (1680 × 1680 μm) and then subtracting the smoothed image from the original image to remove low frequency spatial components. Response amplitudes were measured in restricted regions (templates) of the imaged field to exclude areas that were either non-responsive or contaminated by large vascular patterns or other artifacts.

Orientation and SF preference maps were constructed as described previously (Issa et al., 2000). Orientation preference maps (angle maps) were calculated using the standard vector-averaging method (Blasdel & Salama, 1986). SF preference was measured at each pixel's preferred orientation (selected from four orientations: 0°, 45°, 90°, and 135°). An SF tuning curve was generated for each pixel from the responses at its preferred orientation. The 'average SF tuning curve' for a large region of cortex was calculated by averaging SF tuning curves from all the pixels in that region. For average AFI and ISI tuning curves the Pearson correlation coefficient was calculated using measured values ($N = 6$ SFs) and p-values are reported for the null hypothesis that the R^2 value for the correlation equals zero.

To compare maps of SF preference generated by ISI and AFI procedures, we first aligned the AFI and ISI orientation maps for each experiment. This was necessary because of small shifts that occur between imaging runs. Alignment was carried out by maximizing the correlation between ISI and AFI orientation preference maps over a 10 × 10 pixel window corresponding to 240 × 240 μm of cortex (orientation maps for all experiments are shown in Supplementary figure 1). Note that this alignment procedure is independent of the SF maps, and as such would not bias any relationships between them.

To determine if the maps generated by ISI and AFI are statistically similar within templated regions, we estimated the preferred SF of a pixel by interpolating responses near the frequency that best activated the pixel [as in (Issa et al., 2000)]. We then calculated the difference in SF preference between each pixel of the two measured maps ("Measured Difference"). This distribution was then compared to the distribution expected if the spatial organization of the SF maps were different but the maps shared the same range of spatial frequencies ("the null hypothesis"). The distribution for the null hypothesis was generated by shuffling the location of pixels in the ISI SF map and calculating the difference between the shuffled ISI map and the AFI SF map ("Shuffled Difference"; the shuffled difference was calculated from the average of 100 pseudo-random shuffles). This procedure maintains the overall distribution of SF preferences, but assumes they are not spatially organized.

We used the Kolmogorov–Smirnov non-parametric test to determine if the "Measured Difference" and "Shuffled Difference" were drawn from the same distribution. If the difference between the measured AFI and ISI maps was significantly smaller than the difference between the measured AFI map and the shuffled ISI map then we concluded that the measured maps were more similar than expected by chance.

A similar Kolmogorov–Smirnov analysis was performed to compare SF tuning curves measured using the two techniques. Pearson correlation coefficients were first calculated for AFI and ISI tuning curves measured at each pixel in the templated area. The distribution of measured correlation coefficients was compared to the distribution for the null hypothesis that the correlation between AFI and ISI tuning curves is due to similar average SF tuning curves over the entire region, not due to the spatial structure of the SF maps. The distribution of the null hypothesis was determined by calculating correlation coefficients after shuffling pixel locations in the ISI images.

The signal-to-noise ratio (SNR) of a data set was estimated as follows. For a given spatial frequency, the signal strength was defined as the variance of pixel intensity in response to the stimuli (averaged over four orientations). The noise level is estimated from the variance in response to a stimulus that produced minimal modulation of cortical activity (we used the response to 1.5 c/° gratings averaged over four orientations, which had the lowest variance in all experiments). The SNR is calculated as the ratio of the signal at the optimal spatial frequency to the noise.

Because we were testing the similarity of maps across modalities within a single imaged field, rather than similarity of maps across animals, statistical tests of similarities were performed on each pair of maps (ISI and AFI maps). The number of samples (N) in the Kolmogorov–Smirnov tests is therefore equal to the number of pixels in a templated field.

3. Results

We used two independent techniques to map SF preference in cat Area 17 by measuring optical responses to sinusoidal gratings with different spatial frequencies. Fig. 1 shows an example of responses to a single grating using AFI and ISI. In these images, bright areas represent patches of cortex that are activated by the stimulus, while dark areas are inactive (Fig. 1B and C). As has been observed in previous intrinsic signal imaging studies (Everson

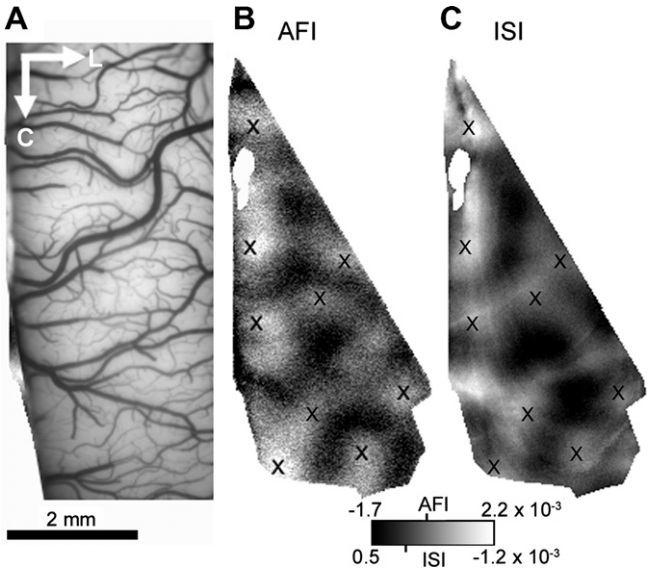

Fig. 1. AFI and ISI responses to a sinusoidal grating. (A) The lateral gyrus imaged under green light to highlight the vascular pattern. (B) Response to a 0.5 c/°, horizontal sinusoidal grating imaged with flavoprotein autofluorescence; active regions appear bright. (C) Response to the same stimulus imaged with intrinsic signal imaging. For comparison with (B), the image intensities have been inverted to make bright areas represent stronger cortical activity. "X"s mark the same locations in (B) and (C). The grayscale bar shows the amplitude of responses ($\Delta F/F$ for AFI and $\Delta R/R$ for ISI), with the 0-points marked by short vertical lines.

et al., 1998; Hubener et al., 1997; Issa et al., 2000; Shoham et al., 1997a), sinusoidal gratings activate restricted regions within Area 17. The same regions appear active with both imaging techniques, consistent with previous comparisons of AFI and ISI responses to square wave gratings (Husson et al., 2007).

The intensity and pattern of cortical autofluorescence varied with spatial frequencies ranging between 0.25 and 1.0 c/°, similar to the range of SF preferences found in neurons of cat Area 17 using single-unit electrophysiology (Movshon et al., 1978; Tolhurst & Thompson, 1981). As Fig. 2 shows, the average SF tuning curve in Area 17 was similar when measured with either AFI or ISI (Fig. 2A: Pearson correlation coefficient $R = 0.84$, $p = 0.04$, $N = 6$ for all comparisons; peak SF from log-Gaussian fit, AFI = 0.49 c/°, ISI = 0.38 c/°, Fig. 2B: $R = 0.98$, $p = 0.0006$; peak SF, AFI = 0.35 c/°, ISI = 0.35 c/°; Supp. Fig. 2A: peak SF, AFI = 0.30 c/°, ISI = 0.30 c/°, $R = 0.84$, $p = 0.04$; Supp. Fig. 2B: $R = 0.82$, $p = 0.04$; peak SF, AFI = 0.32 c/°, ISI = 0.32 c/°) suggesting that the techniques are reporting similar overall patterns of cortical responses. Both the AFI and ISI images are therefore consistent with previous electrophysiological and imaging studies that showed that Area 17 is selective for a narrow band of spatial frequencies (Issa et al., 2000; Movshon et al., 1978; Tolhurst & Thompson, 1981).

3.1. Are the SF maps produced by AFI and ISI similar?

To determine if the AFI and ISI maps of SF preference had similar spatial organizations, we compared SF maps generated from responses to 24 sinusoidal gratings, each with a unique combination of orientation and spatial frequency. Fig. 3 shows AFI and ISI SF preference maps, in which the brightness of each pixel represents the SF that best activated it (brighter pixels represent a higher preferred SF; Supp. Fig. 3 shows two other examples). Both the AFI and ISI maps show that the cortex is tiled with domains that prefer different spatial frequencies.

The structure of the maps generated by the two techniques is similar, although not identical. To determine how similar the two maps are, we calculated the point-by-point difference in SF preference determined from the two measurement methods. If AFI and ISI indicate that a given pixel responds best to the same spatial frequency then the difference in SF preference for that pixel is zero. Because of noise in the measurements it is unlikely that measured SF preferences will be exactly the same between the imaging modalities, but if many pixels have small differences in measured preference then the maps measured by the two modalities must be similar. Fig. 4A shows histograms (solid lines) of differences in SF preference measured by AFI and ISI ("measured differences") for two experiments (Supp. Fig. 4 shows measurements from the other two cases). The difference in SF preference measured by the two techniques was less than the average sampling interval (0.3 c/°) for at least 60% of the pixels in each experiment (mean ± *SD* of 67 ± 7%, $N = 4$). Thus, most of the pixels had similar SF preferences when measured by AFI and ISI, suggesting that the SF preference map measured by AFI is similar to the map measured by ISI.

3.2. Are the SF preference maps more similar than expected by chance?

We would expect a high degree of similarity between the AFI and ISI maps simply because the distribution of SF preferences is peaked between 0.3 and 0.6 c/° (as shown by the log-Gaussian distributions for AFI and ISI average tuning curves in Fig. 2). As a consequence, the calculated differences between SF maps would be small, even if the structure of the maps were very different. Consider for example if 80% of pixels preferred horizontal orientations in an orientation preference map—most pixels would prefer the same stimulus orientation even if there were no structure to the map. A more stringent test for spatial organization, therefore, is to determine if the maps are more similar than would be expected if there were no structure in the maps. The specific "null hypothesis" is that the ISI and AFI SF maps appear similar because they share a similar overall distribution of SF preferences, not because their SF maps have similar structures. To rule out this null hypothesis we therefore compared the measured AFI maps to shuffled ISI maps. Shuffling a map disrupts the spatial structure but does not affect the overall distribution of SF preferences. If the measured AFI map is more similar to the measured ISI map than it is to the shuffled ISI map, then we would conclude that two measured SF maps share similar structures.

As the histograms in Fig. 4A and B show, the shuffled ISI maps are less like the AFI maps than the measured ISI maps (measured map distribution is compared to the average distribution from 100 shuffled ISI maps). Specifically, the population of differences in SF preferences between the AFI and shuffled map is shifted to higher values. To determine if the shuffled distribution of differences is significantly greater than the measured distribution, we replotted both as cumulative distributions (Fig. 4C and D) and measured the greatest distance between them (the "K–S Statistic" labeled in Fig. 4D). If the K–S statistic is greater than a reference distance specified by the Kolmogorov–Smirnov test, the distributions are considered significantly different. The difference between the shuffled maps and AFI maps was significantly greater than the difference between the measured AFI and ISI maps in all four experiments ($p < 0.01$; bin size = 0.01 c/°, the number of pixels, *N*, is specified for each case in the legend of Fig. 4C and D and Supp. Fig. 4C and D). This rules out the null hypothesis, and suggests that in addition to similar distributions of SF preference, the maps also have similar spatial structures.

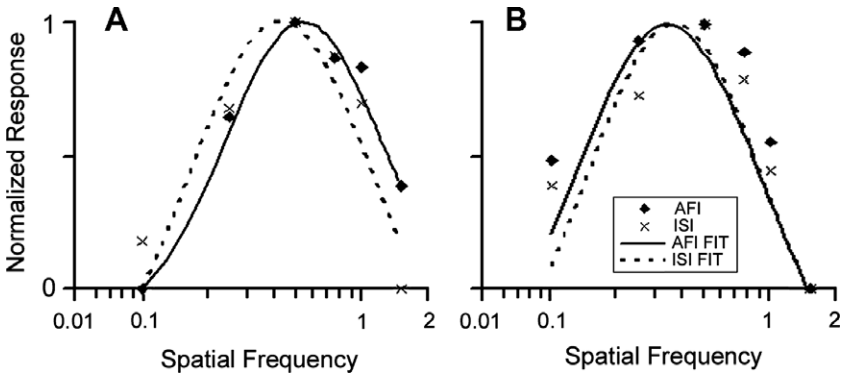

Fig. 2. Spatial frequency distributions measured by AFI and ISI. (A) Average SF tuning curve for the imaged area in Fig. 1. The lines show the best log-Gaussian fit to the data (solid line: AFI; dashed line: ISI). (B) SF tuning curves from a different animal (imaged field shown in Fig. 3C and D).

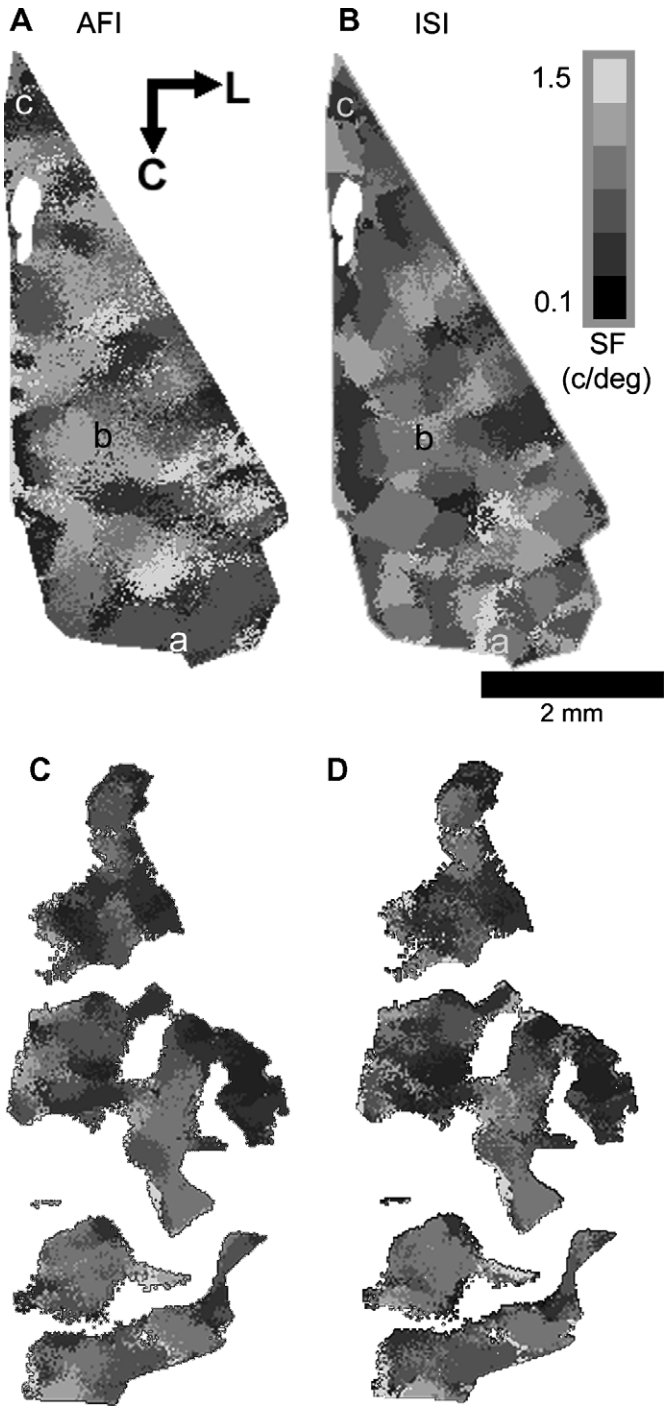

Fig. 3. Spatial frequency maps measured by AFI and ISI. (A) SF map of cat Area 17 generated using AFI (same imaged field as Fig. 1). SF preference is represented by pixel brightness, in which dark pixels prefer low spatial frequencies and bright pixels prefer high spatial frequencies. The lower case letters a, b and c in the imaged field indicate the pixels at which the tuning curves were generated in Fig. 6A–C. (B) SF map in the same imaged field generated using ISI. (C) AFI SF map from a different animal (Same field as Fig. 2B). (D) ISI SF map in the same imaged field as (C).

While the above analysis shows that the measured distribution is different from the average of 100 shuffled distributions, it is still possible that a substantial fraction of 100 randomly shuffled maps might be similar to the measured maps. To rule this out, we estimated the variability of the measurements within the shuffled distributions. In Fig. 5A we consider the average difference between the SF preference measured in AFI and ISI maps. For the experiment shown in Fig. 3A and B, the average difference in SF preference between the measured AFI and ISI SF maps is 0.317 c/°. By comparison, the average difference between the AFI map and 100 shuffles of the ISI map is 0.368 c/°. Importantly, the range of differences between the AFI map and the shuffled ISI maps was 0.364–0.372 c/°, with a standard deviation of 0.0015 c/°. The difference measured between the AFI and ISI maps is therefore 34 standard deviations less than the difference between the measured AFI map and the 100 shuffles of the ISI map. For the other three cases the difference between the measured and shuffled values were even larger (>40 standard deviations).

Similarly, we considered the fraction of pixels in the measured maps that had a small difference in preferred spatial frequency (within 0.3 c/°, Fig. 5B). For the maps shown in Fig. 3A and B, 60% of the pixels were within 0.3 c/°. When the AFI map was compared to a hundred shuffled maps, the fraction of pixels with small differences was 51%, with a standard deviation of 0.3%. The value from the measured maps is therefore 28 standard deviations greater than the value from the comparison of AFI to shuffled maps. Again, the difference between measured and shuffled values was even greater in the other three cases (>36 standard deviations). Given the large distances between the measured and shuffled values, it is highly unlikely ($p << 0.001$) that the measured maps are drawn from a population of maps in which spatial frequency preferences are organized randomly across the cortical surface.

3.3. Are the SF tuning curves for each pixel more similar than expected by chance?

The similarity between AFI and ISI data from the same animals was not restricted to the peak responses (SF preferences): tuning curves for individual pixels were also significantly more similar than expected from a random distribution. Example SF tuning curves from three pixels are shown in Fig. 6. In these examples, the AFI and ISI tuning curves are positively correlated with each other even in cases in which they do not share the same peak (Pearson correlation coefficient $R = 0.46$ for Fig. 6A, 0.39 for Fig. 6B, 0.61 for Fig. 6C; note that these points were not selected to show the best matching AFI and ISI tuning curves, but have correlation coefficients near the median for the populations). The distributions of the correlations shown in Fig. 7 demonstrate that ISI and AFI SF tuning curves were positively correlated over much of the imaged field (Fig. 7A: mean correlation coefficient = 0.32, median = 0.39; Fig. 7B: mean = 0.48, median = 0.62; Supp. Fig. 5A mean = 0.28, median = 0.39; Supp. Fig. 5B, mean = 0.32, median = 0.42 both mean and median value are reported because the distributions are not Gaussian).

As was the case with SF preference, the similarity in tuning curves might result from the similar distributions of SF preference in cat Area 17. Similar to the argument made in Fig. 4, we compared AFI spatial frequency responses with pixels from the ISI data set randomly shuffled within the templated region. This allowed us to rule out the null hypothesis: that the similarity in SF tuning curves is due to a restricted range of spatial frequency preferences, not to a point-by-point similarity between SF tuning curves. The distribution of correlations between AFI and shuffled-ISI tuning curves is significantly lower than the distribution using the unshuffled ISI maps in all four experiments (dashed lines in Fig. 7; Kolmogorov–Smirnov, $p < 0.01$; bin size = 0.01, N given for each experiment in legend of Fig. 7 and Supp. Fig. 5). As with SF preference, therefore, the SF tuning curves generated by AFI are more similar to their corresponding ISI tuning curves than expected from a randomized distribution of responses. This suggests that the similarity in tuning curves on a pixel-by-pixel basis cannot be explained by the restricted range of spatial frequency prefer-

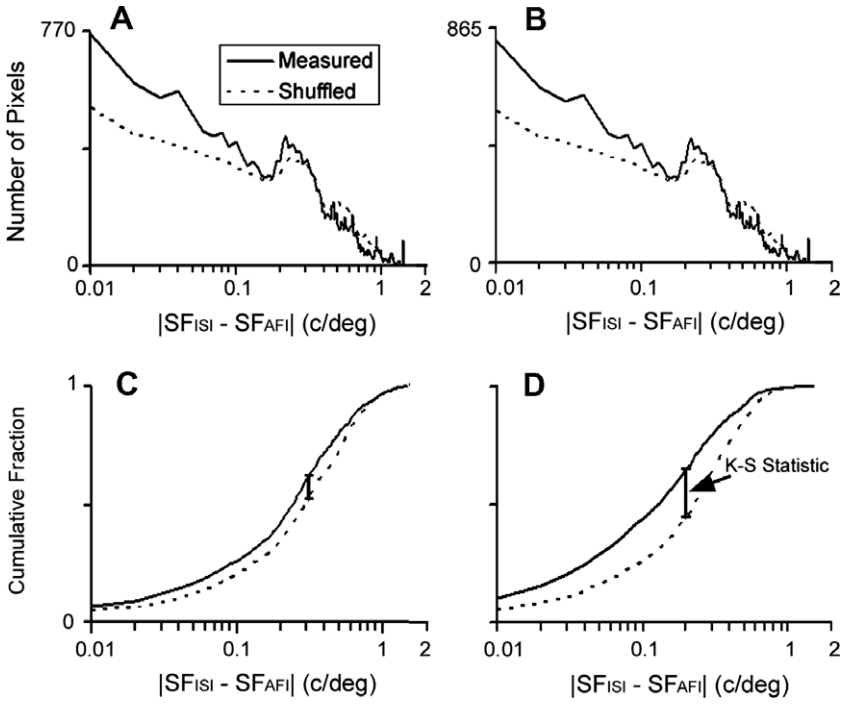

Fig. 4. Distribution of differences between ISI and AFI spatial frequency preference. (A) A histogram of differences in SF preferences measured by ISI and AFI (data from field shown in Fig. 3A and B). SF_{ISI} = SF preference measured by intrinsic signal imaging, SF_{AFI} = preference measured by autofluorescence. The first bin includes all points with a SF preference difference less than 0.01 c/deg, including those with no difference (bin size: 0.01 c/deg). The dashed line shows the difference histogram after the pixels in the ISI map were randomly shuffled. (B) Difference histograms from the fields shown in Fig. 3C and D. (C) Cumulative histograms of the measured difference between the AFI and ISI spatial frequency maps (solid line) and difference between the AFI and shuffled ISI maps (dashed line) for the experiment shown in Fig. 3A and B. The line between the solid and dashed histograms shows the "K–S statistic" (the greatest distance between the measured and shuffled cumulative distributions) used in subsequent analyses. N = 20798 pixels. (D) Cumulative histograms for the experiment shown in Fig. 3C and D. N = 13651 pixels.

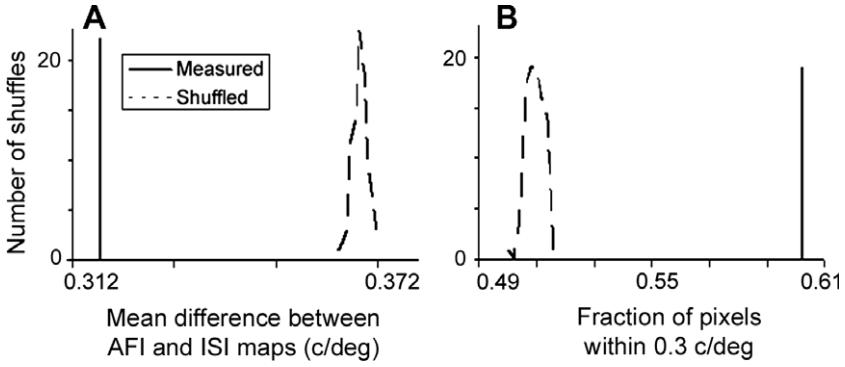

Fig. 5. Variability in shuffled distributions for the experiment shown in Fig. 3 A and B. (A) Histogram of the average difference in SF preference between the AFI map and 100 shuffles of the ISI map (dashed line). The measured difference between AFI and ISI maps is shown for comparison (solid line). (B) Histogram of the fraction of locations that have a spatial frequency preference within 0.3 c/° for the AFI map and 100 shuffles of the ISI map (dashed line). The fraction of locations in the ISI map that are within 0.3 c/° of the AFI map is shown for comparison (solid line).

ences in Area 17, but instead must be due to a similarity in the spatial frequency responses measured by AFI and ISI.

3.4. How consistent are the results across experiments?

We first asked if four experiments were sufficient to conclude that the measured maps are more similar to each other than expected by chance. We compared the four measured K–S statistic values (ranging from 0.09 to 0.21, with mean ± *SD* of 0.15 ± 0.05) to the K–S statistic expected if the maps measured by ISI and AFI were completely unrelated (this is the same as comparing the distance between the shuffled distribution and itself, and the K–S statistic for such a comparison is 0). The distribution of measured K–S statistics was significantly different from 0 at the $p < 0.01$ level (one-sample, one-tailed T-test, $N = 4$, degrees of freedom = 3, $p = 0.003$). The four experiments are therefore sufficient to conclude that the two imaging modalities reveal the same underlying spatial frequency maps.

We next asked if the variability among the data sets could be explained by the variations in the quality of the data among the experiments. If there is an underlying map of spatial frequency preference, we would expect the difference between measured and shuffled maps (the K–S statistic) to increase with the quality of the data (signal-to-noise ratio). As Fig. 8 shows, the difference between measured and shuffled maps increased with the signal-to-noise ratio of AFI responses (linear correlation $R = 0.95$, $N = 4$,

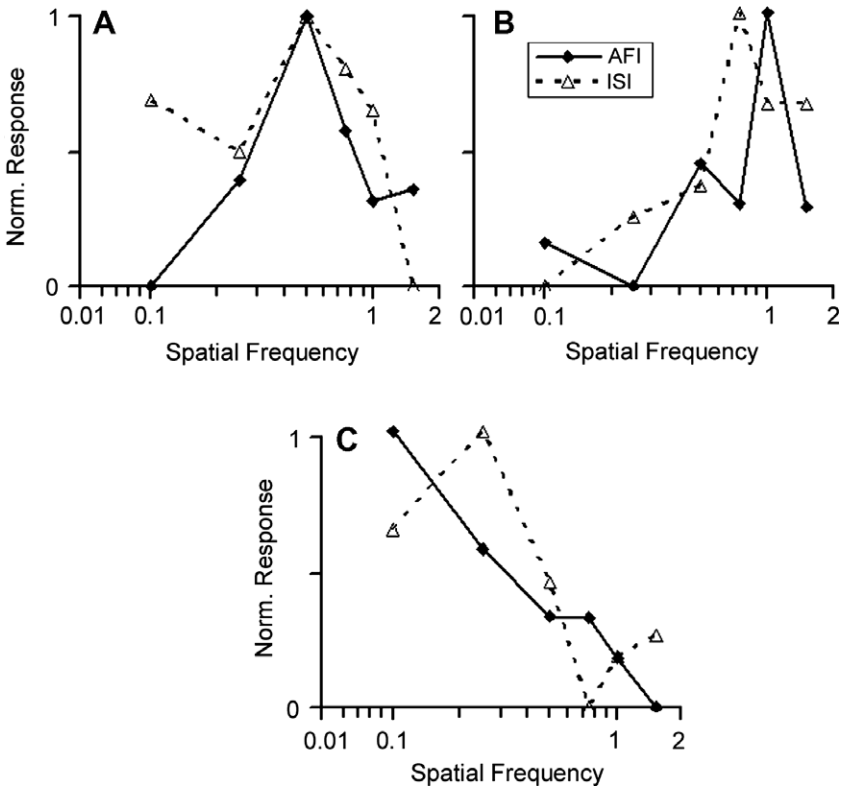

Fig. 6. Spatial frequency tuning curves for three pixels measured by ISI and AFI. (A) AFI and ISI tuning curves for a pixel at which the SF preferences are the same ($pSF_{AFI} = pSF_{ISI} = 0.50$ c/deg; $R = 0.46$). (B) Tuning curves for a pixel with the median correlation value for the experiment in Fig. 3A and B ($pSF_{AFI} = 1.0$; $pSF_{ISI} = 0.75$; $R = 0.39$). (C) Tuning curves for another pixel in the imaged field ($pSF_{AFI} = 0.1$; $pSF_{ISI} = 0.25$; $R = 0.61$). The locations of the pixels are indicated in Fig. 3A and B.

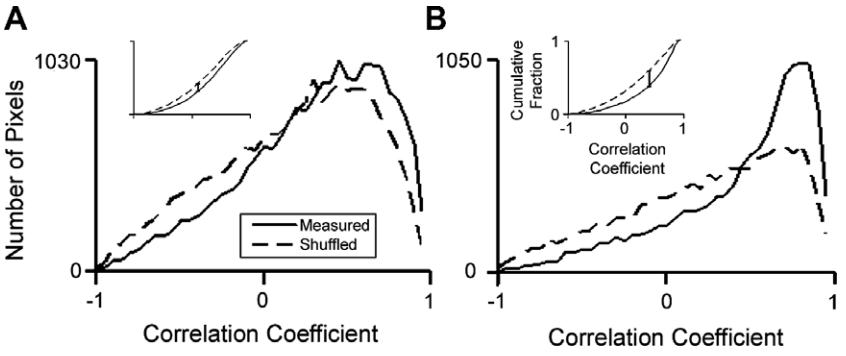

Fig. 7. Distribution of correlations between ISI and AFI tuning curves. (A) A histogram of Pearson correlation coefficients between ISI and AFI tuning curves for the pixels in the templated region of the maps shown in Fig. 3A and B. The dashed line shows the correlation coefficients after the pixel locations in the ISI map were randomly shuffled. (Measured: mean correlation coefficient = 0.32, median = 0.39; Shuffled: mean correlation coefficient = 0.21, median = 0.27) Inset: A cumulative histogram of the Pearson correlation coefficients shown in the main figure. $N = 20798$ pixels. (B) Histograms from the experiment shown in Fig. 3C and D. (Measured: mean correlation coefficient = 0.47, median = 0.60; Shuffled: mean correlation coefficient = 0.26, median = 0.34). $N = 13651$ pixels.

$p = 0.05$, accounts for 90% of variance). In contrast, the signal-to-noise ratio of ISI responses was unrelated to the K–S statistic ($R = 0.25$, $N = 4$, $p > 0.05$, accounts for only 6% of variance with an inverse relationship), consistent with the observation that the SNR for ISI images was on average 1.4× that of AFI images. Together, these results suggest that the AFI signal, not the ISI signal, was the limiting factor in data quality. The strong relationship between the AFI signal-to-noise ratio and the K–S statistic explains most of variability in the measurements of similarity between the AFI and ISI spatial frequency maps in the different experiments.

If the two imaging modalities are capturing the same underlying spatial frequency map, then repeated measurements with a single modality should produce similar results as imaging with two separate methods. In two experiments we were able to compare repeated mappings of spatial frequency preference using AFI. As with the comparison between AFI and ISI maps, the comparison of repeat maps shows that they are more similar than expected by chance (Fig. 9). Since the AFI signal has a lower signal-to-noise ratio than does ISI, however, we would expect the repeated AFI maps to be less similar to each other than the AFI and ISI maps are. Consistent with this expectation, the K–S statistics for repeat maps, while statistically significant ($p < 0.01$, binsize = 0.01c/°, Fig. 9B, $N = 13651$, from same animal as shown in Fig. 3C and D; Fig. 9C, $N = 10900$, from same animal as shown in Supp. Fig. 3C and D), are smaller than the K–S statistic for the associated AFI-ISI comparison (experiment 1: K–S statistic for AFI to ISI compari-

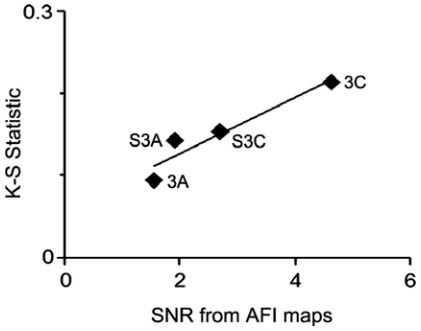

Fig. 8. Similarity measure increases with AFI signal-to-noise ratio. The K–S statistic for each of the four experiments is plotted against the signal-to-noise ratio from the AFI map from that experiment (Fig. 4 and Suppl. Fig. 4). The linear fit (solid line) accounted for 93% of the variance in data ($R = 0.97$). Next to each marker is the number of the figure in which the associated AFI SF map is shown.

son = 0.21, repeat AFI measurements K–S statistic = 0.15; Experiment 2: K–S statistic AFI to ISI = 0.15, repeat AFI K–S statistic = 0.11). This suggests that, given the signal-to-noise ratio of AFI, the two different techniques are producing maps as similar as possible.

One additional concern is that the templating procedure used to exclude weakly responding areas and vasculature might artifactually bias the maps to contain only regions that are similar across AFI an ISI methods. We have therefore reanalyzed all the maps using templates in which any portion of Area 17 that was in the focal plane was included. The two cases that had the most substantial templating are shown in Suppl. Fig. 6. In the first case (experiment shown in Fig. 3C and D) the template was drawn conservatively to exclude blood vessels. When the template was expanded (as shown in Supp. Fig. 6B) the similarity between the AFI and ISI SF maps (the K–S statistic) was smaller but remained statistically significant (K–S Statistic, original template = 0.21, K–S Statistic, expanded template = 0.13; expanded template: $p < 0.01$, bin size = 0.01 c/°, $N = 22298$ pixels, Supp. Fig. 6I). In the second case (experiment shown in Suppl. Fig. 3A and B) the template was drawn to exclude a region in which responses were weak based on noise in the orientation map (see the orientation map in Suppl. Fig. 6F). When the template was expanded to include the noisy area the similarity between the AFI and ISI maps decreased (Supp. Fig. 6J) but again the difference between the measured and shuffled distributions remained statistically significant (K–S Statistic, original template = 0.14, K–S Statistic, expanded template = 0.12; expanded template: $p < 0.01$, bin size = 0.01 c/°, $N = 31484$ pixels, Supp. Fig. 6J). Therefore the observed similarity between the AFI and ISI SF maps is robust regardless of the detailed pattern of the template used to exclude artifacts.

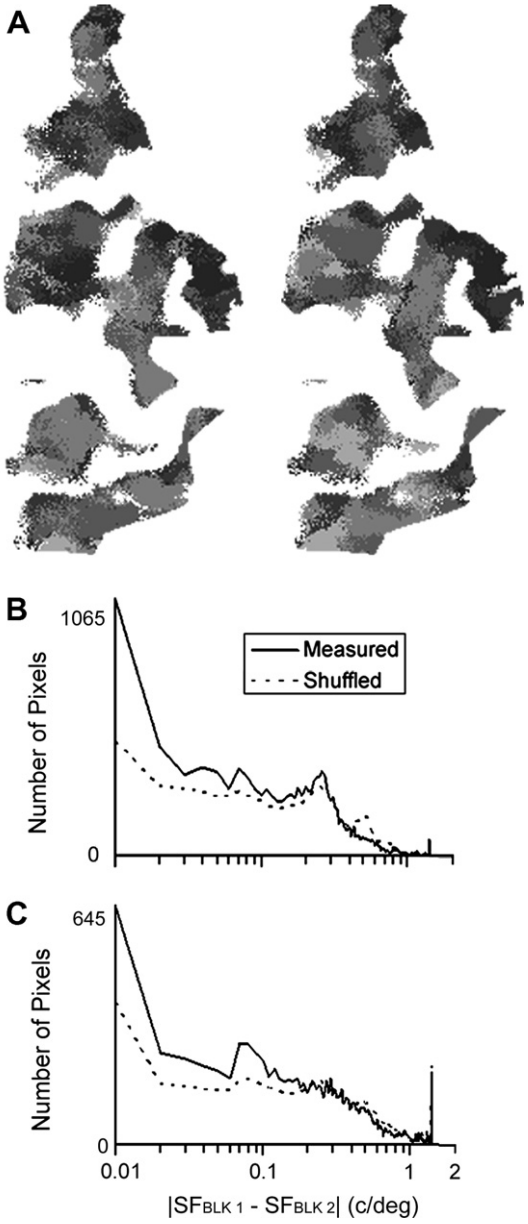

Fig. 9. Repeated mapping of spatial frequency preference with AFI. (A) AFI SF preference maps from two separate blocks of 16 stimulus repetitions from the experiment shown in Fig. 3C and D (the map in Fig. 3C is an average of these two blocks). (B) Histogram of differences in SF preferences between block 1 and block 2 from the data shown in (A). The solid line shows the difference histogram between measured AFI maps in block 1 and block 2, while the dashed line shows the difference histogram after the pixels in block 2 were randomly shuffled. (C) Histogram of differences between block 1 and block 2 for the experiment shown in Supp. Fig. 3C and D.

4. Discussion

In previous studies, intrinsic signal imaging provided evidence for a tangential organization of spatial frequency preference in cat primary visual cortex, but the structure of ISI SF maps has been called into question because of their susceptibility to vascular artifacts. Specifically, reanalysis of data from previously published experiments (Everson et al., 1998; Issa et al., 2000) suggested that ISI SF maps might represent vascular patterns rather than neuronal SF preferences, and new data from an additional animal was used to argue that SF preference is not clustered in Area 17 (Sirovich & Uglesich, 2004). To address the organization of SF preference using a non-hemodynamic imaging method, we mapped SF map structure in Area 17 with AFI and compared the observed structure to that found by ISI. Both ISI and AFI imaging techniques generate maps containing domains with specific SF preferences, and AFI and ISI SF maps and tuning curves were statistically similar in structure. Because autofluorescence imaging is far less affected by vascular artifacts than intrinsic signal imaging (Husson et al., 2007), the similarity between SF maps produced by AFI and ISI provide a strong argument that the clustering of SF preference is not a vascular artifact but rather is a genuine feature of the organization of Area 17.

The SF response properties presented here might also be reconciled with those found by Sirovich and Uglesich. In that study, two methods were used to analyze SF maps. The first was to fit the SF tuning curve of each point on the cortical surface with a combina-

tion of two independent basis functions modeled on inputs from X cells (being selective for high SFs) and inputs from Y cells (being selective for low frequencies) (Sirovich & Uglesich, 2004). While the authors suggested that the ability to fit tuning curves with two basis functions means there is no variation in spatial frequency preference, such combinations of basis functions can actually produce unimodal response profiles with peaks at a variety of different SFs depending on the relative weighting of the functions. This is analogous to the orientation preference map, which shows a wide range of orientation preference, but the responses at any single pixel can be fit to a sum of two basis functions (for orientation tuning these basis functions are sine and cosine functions). Such fitting produced a map of relative weights for the two basis functions that appears to have clusters (Sirovich and Uglesich Fig. 5)—there are domains dominated by the lower SF component, domains dominated by the higher SF component, and domains in which the weights are nearly equal. This distribution is much like the organization of SF preference observed here and elsewhere (Everson et al., 1998; Hubener et al., 1997; Issa et al., 2000; Shoham, Hubener, Schulze, Grinvald, & Bonhoeffer, 1997b), and is therefore consistent with our finding that there is a range of SF preferences distributed across the cortical surface.

Their second approach was an attempt to remove "non-stimulus specific" responses that might contaminate maps. Sirovich and Uglesich reanalyzed one data set from Issa et al. (2000) using this approach. To reduce the effect of "non-specific" responses, images were averaged over all orientations and then the average was subtracted from each single-condition image. This was based on the unwritten assumption that all stimulus-specific responses must be tuned for orientation. After this subtraction, the response patterns generated by high spatial frequency stimuli appeared similar to those generated in response to low spatial frequency stimuli. The similarity between the two patterns led the authors to conclude that there are not different spatial frequency domains, but rather that the remaining patterns in the spatial frequency map were more closely related to vascular patterns. The problem with this analysis is that not all stimulus-specific responses are strongly tuned for orientation. In particular, low and high spatial frequency domains tend to co-localize with orientation pinwheels (Hubener et al., 1997; Issa et al., 2000, and Fig. 4 of Sirovich & Uglesich, 2004), which appear poorly oriented in optical maps even though individual neurons are sharply tuned (Maldonado, Godecke, Gray, & Bonhoeffer, 1997; Ohki et al., 2006). Because the subtraction procedure removes activity in poorly oriented regions, it preferentially reduces responses in low and high spatial frequency domains, accentuating activity in intermediate spatial frequency domains and artifactually degrades the spatial frequency map.

The autofluorescence maps of SF preference directly confirm that the organization of SF seen by intrinsic signal imaging is not due to vascular artifacts. Several features of the autofluorescence signal suggest that it is relatively free of vascular artifacts. First, the autofluorescence signal is thought to derive from mitochondrial flavoproteins, so it is unrelated to the vascular pattern (Reinert et al., 2004). Second, blood vessel fluorescence does not change with cortical activity; therefore, blood vessels do not appear to respond preferentially to visual stimulation as they do with intrinsic signal imaging (Husson et al., 2007). Finally, autofluorescence has excellent spatial resolution because it lacks the long-range spatial correlations found in intrinsic signal imaging. For example, the average size of orientation domains is 30% smaller in single-condition autofluorescence images than in intrinsic signal images (Husson et al., 2007). Because the autofluorescence and intrinsic signal imaging techniques are independent, they provide complementary support for the organization of SF preference in cat Area 17.

Despite the similarities in overall structure, the match between the AFI and ISI SF maps is weaker than the match between orientation maps generated by the same techniques. The differences between SF and orientation maps can be attributed to two sources. First, AFI and ISI responses to sinusoidal gratings are weaker than responses to the square wave gratings typically used to map orientation preference. Square wave gratings, which contain many spatial and temporal frequencies, activate multiple SF domains at once, and because each SF domain has a moderately broad SF tuning curve, each SF domain is more strongly activated by the multiple SFs in the square wave than they are by the single SF in a sine wave grating. Second, there is less scatter in the neural organization of orientation preference than in the organization of spatial frequency preference. Electrophysiological recordings show that neighboring neurons are more likely to share the orientation preference than spatial frequency preference (DeAngelis & Newsome, 1999). The net effect is that SF maps are noisier than orientation maps.

That the two imaging methods are subject to different artifacts also contributes to the apparent differences between the ISI and AFI SF maps. Even with the use of templates to exclude large blood vessels, not all vasculature can be excluded from the maps. As a result, an ISI map will have vascular artifacts that make it different from the AFI map. Similarly, because the autofluorescence signal lacks the long-range spatial correlations found with intrinsic signals, the AFI maps appear more pixilated ("noisier") than the ISI maps. The statistically significant relationship between the ISI and AFI SF maps, despite low-amplitude responses and different artifacts in the two techniques, suggests that there is an underlying organization of SF preference in Area 17.

With these new results from autofluoresence imaging, a growing body of evidence converges on the notion that SF preference is mapped systematically across the cortical surface: electrophysiological and 2-DG anatomical studies suggest that cortical neurons are clustered by SF preference (DeAngelis et al., 1999; Issa et al., 2000; Shoham et al., 1997b; Thompson & Tolhurst, 1979a, 1979b; Tolhurst & Thompson, 1982), while intrinsic signal imaging has revealed an organization to SF preference in Area 17 of cats (Everson et al., 1998; Hubener et al., 1997; Issa et al., 2000; Shoham et al., 1997b), ferrets (Basole, White, & Fitzpatrick, 2004; Yu, Farley, Jin, & Sur, 2005) and the bush baby (Xu, Anderson, & Casagrande, 2007). Moreover, intrinsic signal imaging has also shown that responses to complex images are decomposed into SF domains based on the SFs in the image (Zhang, Rosenberg, Mallik, Husson, & Issa, 2007). Here, the response maps generated by flavoprotein autofluorescence imaging confirm that SF preference varies over the surface of Area 17.

Acknowledgments

We thank members of the Issa lab for helpful comments on the manuscript. This work was supported by grants from the NIH T32GM07281 (A.K.M.), DHS Fellowship DE-AC05-00OR22750 (A.R.), the Brain Research Foundation, the Sloan Foundation and the Mallinckrodt Foundation (N.P.I.).

Appendix A. Supplementary data

Supplementary data associated with this article can be found, in the online version, at doi:10.1016/j.visres.2008.04.014.

References

Basole, A., White, L. E., & Fitzpatrick, D. (2004). Mapping of spatial and temporal frequency preference in ferret visual cortex. *Society for Neuroscience*, 410–415.

Blasdel, G. G., & Salama, G. (1986). Voltage-sensitive dyes reveal a modular organization in monkey striate cortex. *Nature, 321*(6070), 579–585.

Bonhoeffer, T., & Grinvald, A. (1996). Optical imaging based on intrinsic signals. In A. W. Toga & J. C. Mazziotta (Eds.), *Brain mapping: The methods* (pp. 55–97). New York: Academic Press.

Brainard, D. H. (1997). The psychophysics toolbox. *Spatial Vision, 10*(4), 433–436.

Campbell, F. W., Cooper, G. F., & Enroth-Cugell, C. (1969). The spatial selectivity of the visual cells of the cat. *Journal of Physiology, 203*(1), 223–235.

DeAngelis, G. C., Ghose, G. M., Ohzawa, I., & Freeman, R. D. (1999). Functional micro-organization of primary visual cortex: Receptive field analysis of nearby neurons. *Journal of Neuroscience, 19*(10), 4046–4064.

DeAngelis, G. C., & Newsome, W. T. (1999). Organization of disparity-selective neurons in macaque area MT. *Journal of Neuroscience, 19*(4), 1398–1415.

Everson, R. M., Prashanth, A. K., Gabbay, M., Knight, B. W., Sirovich, L., & Kaplan, E. (1998). Representation of spatial frequency and orientation in the visual cortex. *Proceedings of the National Academy of Sciences of the United States of America, 95*(14), 8334–8338.

Foster, K. A., Galeffi, F., Gerich, F. J., Turner, D. A., & Muller, M. (2006). Optical and pharmacological tools to investigate the role of mitochondria during oxidative stress and neurodegeneration. *Progress in Neurobiology, 79*(3), 136–171.

Hubel, D. H., & Wiesel, T. N. (1962). Receptive fields, binocular interaction and functional architecture in the cat's visual cortex. *Journal of Physiology (London), 160*, 106–154.

Hubener, M., Shoham, D., Grinvald, A., & Bonhoeffer, T. (1997). Spatial relationships among three columnar systems in cat area 17. *Journal of Neuroscience, 17*(23), 9270–9284.

Husson, T. R., Mallik, A. K., Zhang, J., & Issa, N. P. (2007). Functional imaging of primary visual cortex using flavoprotein autofluorescence. *Journal of Neuroscience, 27*(32), 8665–8675.

Issa, N. P., Trepel, C., & Stryker, M. P. (2000). Spatial frequency maps in cat visual cortex. *Journal of Neuroscience, 20*(22), 8504–8514.

Maffei, L., & Fiorentini, A. (1977). Spatial frequency rows in the striate visual cortex. *Vision Research, 17*(2), 257–264.

Maldonado, P. E., Godecke, I., Gray, C. M., & Bonhoeffer, T. (1997). Orientation selectivity in pinwheel centers in cat striate cortex. *Science, 276*(5318), 1551–1555.

Movshon, J. A., Thompson, I. D., & Tolhurst, D. J. (1978). Spatial and temporal contrast sensitivity of neurones in areas 17 and 18 of the cat's visual cortex. *Journal of Physiology, 283*, 101–120.

Ohki, K., Chung, S., Kara, P., Hubener, M., Bonhoeffer, T., & Reid, R. C. (2006). Highly ordered arrangement of single neurons in orientation pinwheels. *Nature, 442*(7105), 925–928.

Pelli, D. G. (1997). The VideoToolbox software for visual psychophysics: Transforming numbers into movies. *Spatial Vision, 10*(4), 437–442.

Reinert, K. C., Dunbar, R. L., Gao, W., Chen, G., & Ebner, T. J. (2004). Flavoprotein autofluorescence imaging of neuronal activation in the cerebellar cortex in vivo. *Journal of Neurophysiology, 92*(1), 199–211.

Shoham, D., Hubener, M., Schulze, S., Grinvald, A., & Bonhoeffer, T. (1997a). Spatio-temporal frequency domains and their relation to cytochrome oxidase staining in cat visual cortex. *Nature, 385*(6616), 529–533.

Shoham, D., Hubener, M., Schulze, S., Grinvald, A., & Bonhoeffer, T. (1997b). Spatio-temporal frequency domains and their relation to cytochrome oxidase staining in cat visual cortex (Vol. 385, p. 529, 1997). *Nature, 386*(6622), 302.

Sirovich, L., & Uglesich, R. (2004). The organization of orientation and spatial frequency in primary visual cortex. *Proceedings of the National Academy of Sciences of the United States of America, 101*(48), 16941–16946.

Thompson, I. D., & Tolhurst, D. J. (1979a). Optimal spatial frequencies of neighbouring neurones in the cat's visual cortex. *Proceedings of the Physiological Society*, 57P.

Thompson, I. D., & Tolhurst, D. J. (1979b). The representation of spatial frequency in cat visual cortex: A 14C-2-deoxyglucose study. *Proceedings of the Physiological Society*, 58P.

Tohmi, M., Kitaura, H., Komagata, S., Kudoh, M., & Shibuki, K. (2006). Enduring critical period plasticity visualized by transcranial flavoprotein imaging in mouse primary visual cortex. *Journal of Neuroscience, 26*(45), 11775–11785.

Tolhurst, D. J., & Thompson, I. D. (1981). On the variety of spatial frequency selectivities shown by neurons in area 17 of the cat. *Proceedings of the Royal Society of London. Series B: Biological Sciences, 213*(1191), 183–199.

Tolhurst, D. J., & Thompson, I. D. (1982). Organization of neurones preferring similar spatial frequencies in cat striate cortex. *Experimental Brain Research, 48*(2), 217–227.

Turner, D. A., Foster, K. A., Galeffi, F., & Somjen, G. G. (2007). Differences in O(2) availability resolve the apparent discrepancies in metabolic intrinsic optical signals in vivo and in vitro. *Trends in Neuroscience, 30*(8), 390–398.

Xu, X., Anderson, T. J., & Casagrande, V. A. (2007). How do functional maps in primary visual cortex vary with eccentricity? *Journal of Comparative Neurology, 501*(5), 741–755.

Yu, H., Farley, B. J., Jin, D. Z., & Sur, M. (2005). The coordinated mapping of visual space and response features in visual cortex. *Neuron, 47*(2), 267–280.

Zhang, J., Rosenberg, A., Mallik, A. K., Husson, T. R., & Issa, N. P. (2007). The representation of complex images in spatial frequency domains of primary visual cortex. *Journal of Neuroscience, 27*(35), 9310–9318.